











ARTICLE

<https://doi.org/10.1038/s41467-019-11128-6>

OPEN

Reduced marine phytoplankton sulphur emissions in the Southern Ocean during the past seven glacials

K. Goto-Azuma ^{1,2}, M. Hirabayashi¹, H. Motoyama ^{1,2}, T. Miyake¹, T. Kuramoto ^{1,8}, R. Uemura ^{1,9}, M. Igarashi¹, Y. Iizuka³, T. Sakurai ^{1,10}, S. Horikawa^{3,11}, K. Suzuki ⁴, T. Suzuki ⁵, K. Fujita ⁶, Y. Kondo ¹, S. Hattori ⁷ & Y. Fujii¹

Marine biogenic sulphur affects Earth's radiation budget and may be an indicator of primary productivity in the Southern Ocean, which is closely related to atmospheric CO₂ variability through the biological pump. Previous ice-core studies in Antarctica show little climate dependence of marine biogenic sulphur emissions and hence primary productivity, contradictory to marine sediment records. Here we present new 720,000-year ice core records from Dome Fuji in East Antarctica and show that a large portion of non-sea-salt sulphate, which was traditionally used as a proxy for marine biogenic sulphate, likely originates from terrestrial dust during glacials. By correcting for this, we make a revised calculation of biogenic sulphate and find that its flux is reduced in glacial periods. Our results suggest reduced dimethylsulphide emissions in the Antarctic Zone of the Southern Ocean during glacials and provide new evidence for the coupling between climate and the Southern Ocean sulphur cycle.

¹National Institute of Polar Research, Research Organization of Information and Systems, 10-3 Midori-cho, Tachikawa, Tokyo 190-8518, Japan. ²Department of Polar Science, Graduate University for Advanced Studies (SOKENDAI), 10-3 Midori-cho, Tachikawa, Tokyo 190-8518, Japan. ³Institute of Low Temperature Science, Hokkaido University, Kita-19, Nishi-8, Kita-ku, Sapporo 060-0819, Japan. ⁴Faculty of Science, Shinshu University, 3-1-1 Asahi, Matsumoto 390-8621, Japan. ⁵Faculty of Science, Yamagata University, 1-4-12 Kojirakawa-cho, Yamagata 990-8560, Japan. ⁶Graduate School of Environmental Studies, Nagoya University, Furo-cho, Chikusa-ku, Nagoya 464-8601, Japan. ⁷Department of Chemical Science and Engineering, School of Materials and Chemical Technology, Tokyo Institute of Technology, Yokohama 226-8502, Japan. ⁸Present address: Department of Human Development, School of Humanities and Culture, Tokai University, 4-1-1 Kitakaname, Hiratsuka 259-1292, Japan. ⁹Present address: Graduate School of Environmental Studies, Nagoya University, Furo-cho, Chikusa-ku, Nagoya 464-8601, Japan. ¹⁰Present address: Civil Engineering Research Institute for Cold Region, Public Works Research Institute, 1-3-1-34, Hiragishi, Toyohira-ku, Sapporo 062-8602, Japan. ¹¹Present address: Earthquake and Volcano Research Center, Graduate School of Environmental Studies, Nagoya University, Furo-cho, Chikusa-ku, Nagoya 464-8601, Japan. Correspondence and requests for materials should be addressed to K.G.-A. (email: kumiko@nipr.ac.jp)

Dimethylsulphide (DMS) emitted from oceanic phytoplankton plays an important role in controlling concentrations of sulphate (SO_4^{2-}) aerosols, which can act as cloud condensation nuclei (CCN)^{1–3}. Changes in CCN would influence cloud albedo, a key parameter of radiative forcing^{1–3}. Increased SO_4^{2-} can thus cool the Earth by indirect forcing, in addition to direct forcing owing to increased scattering of solar radiation³. To understand these effects, DMS emissions and their links to climate should be evaluated in a pristine environment². DMS and its oxidation products, SO_4^{2-} and methanesulphonate (CH_3SO_3^- , hereafter MSA), are also indicators of primary productivity in the Southern Ocean (SO), which is important because they are closely related to atmospheric CO_2 variability through the biological pump⁴. SO_4^{2-} and MSA in Antarctic ice cores are therefore useful tools for investigating links between the sulphur cycle and climate.

High concentrations of non-sea-salt (nss) SO_4^{2-} measured in glacial samples from Vostok ice core drilled in East Antarctica⁵ (Supplementary Fig. 1) have been interpreted as evidence of enhanced oceanic DMS emissions during glacials, assuming that nss SO_4^{2-} is mainly of marine biogenic DMS origin. A subsequent study on the same ice core⁶ reports increased MSA concentrations in addition to nss SO_4^{2-} , further supporting the interpretation of [5] because MSA originates solely from DMS, whereas nss SO_4^{2-} can come from other sources^{7,8}. Based on these results, DMS emissions and hence nss SO_4^{2-} have been believed to exert positive feedback on climate. However, more recent studies refute the positive feedback hypothesis^{7,8}, showing that MSA is modified post-depositionally in the Antarctic interior where accumulation rates are low and does not represent DMS production around Antarctica. Furthermore, two deep ice cores drilled at Dome C (EDC) and Dronning Maud Land (EDML) in East Antarctica (Supplementary Fig. 1) show little change in nss SO_4^{2-} flux over glacial/interglacial cycles^{7–9}, while concentrations increase during glacials. Wolff et al.⁷ point out that increased nss SO_4^{2-} concentrations in ice cores from sites with low accumulation rates (e.g., Vostok, EDC, EDML) are mainly caused by decreased accumulation rates in glacials, and can therefore not be interpreted as evidence of increased atmospheric nss SO_4^{2-} . The nearly constant nss SO_4^{2-} fluxes at EDC and EDML, which face the Indian and Atlantic Ocean sectors of the SO, respectively, have been interpreted to reflect stable DMS emissions and hence stable marine biogenic productivity in the Antarctic Zone (AZ) of the SO over glacial cycles, assuming that the major source of nss SO_4^{2-} is DMS^{7–9}. In contrast, marine sediment records show that export production decreases in the AZ during glacials but increases further north in the Sub-Antarctic Zone (SAZ) of the SO⁴. This implies reduced primary productivity in the AZ but increased primary productivity in the SAZ during glacials. The disparity between ice and marine core records has been attributed to differences in marine organisms that contribute to these records⁷.

The stable sulphur isotopic composition of SO_4^{2-} ($\delta^{34}\text{S}$) provides a useful signature of its origins^{10–12}. The $\delta^{34}\text{S}$ data measured from EDC and Vostok ice cores suggest 4–6‰ lower $\delta^{34}\text{S}$ for the last glacial than for the Holocene and last interglacials, although the data are scattered and sparse¹¹. This has been attributed to isotopic fractionation during transport, as terrestrial contribution of SO_4^{2-} has been assumed to be small¹¹. However, surface snow samples from a latitudinal transect between a coastal station (Syowa) and an interior site (Dome Fuji, hereafter DF, Supplementary Fig. 1) show remarkably uniform $\delta^{34}\text{S}$ in East Antarctica¹³. The results suggest that net isotopic fractionation during long-range transport is insignificant in East Antarctica and thus $\delta^{34}\text{S}$ in the ice cores from the East Antarctic interior can be used to infer source contributions. Lower $\delta^{34}\text{S}$ values in the

last glacial¹¹ might be due to an increased contribution of terrestrial SO_4^{2-} originating from increased terrestrial dust^{7,8}. Consequently, little change in the nss SO_4^{2-} flux over glacial/interglacial cycles^{7–9} can be caused by increased terrestrial sulphate and decreased marine biogenic sulphate.

In this study, we propose this alternative interpretation of nss SO_4^{2-} flux and make a revised calculation of DMS-derived sulphate, using new ice core records obtained at DF, spanning the last 720,000 years^{14,15}. On the basis of the revised calculation, we compare the DMS-derived sulphate record from DF with those from EDC and EDML. We find that DMS-derived sulphate fluxes decrease in glacials, which indicates reduced DMS emissions in the AZ of the SO. This suggests that primary production, as well as export production, decreases during glacials, which is consistent with marine sediment records⁴.

Results

Flux variability and potential sources of nss SO_4^{2-} . We calculated nss Ca^{2+} and nss SO_4^{2-} from Ca^{2+} , Na^+ , and SO_4^{2-} concentrations^{7–9,16} (Supplementary Figs. 2a–c). Low accumulation rates ($<30 \text{ kg m}^{-2} \text{ yr}^{-1}$ in the present day and $<50 \text{ kg m}^{-2} \text{ yr}^{-1}$ throughout the last 720,000 years) (Supplementary Fig. 2d) at DF¹⁴ indicate that the dominant process for aerosol deposition is dry deposition and that the flux, rather than the concentration in ice, better represents the changes in atmospheric aerosol concentration^{7,16}. The flux of nss Ca^{2+} at DF covaries with that at EDC^{7,8} and EDML¹⁶, indicating high and low values during glacials and interglacials, respectively (Fig. 1, Supplementary Fig. 3); fluxes at DF are 2.0 and 0.6 times those at EDC and EDML, respectively.

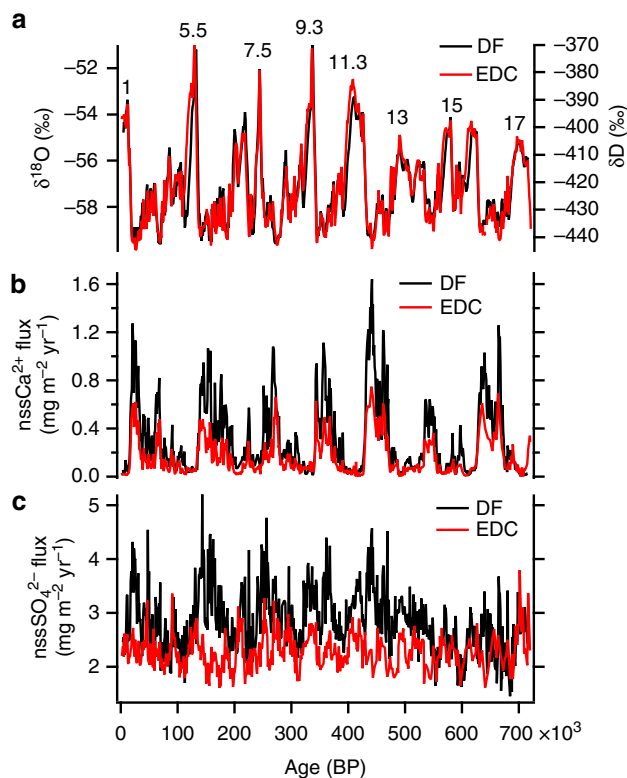


Fig. 1 Temperature proxies and ion fluxes at Dome Fuji (DF) and Dome C (EDC). **a** The $\delta^{18}\text{O}$ (DF)¹⁴ and δD (EDC)^{7,8} records averaged over 1000 years. Marine isotope stage numbers for interglacials are also shown. **b** Fluxes of nss Ca^{2+} at DF and EDC averaged over 1000 years. **c** Fluxes of nss SO_4^{2-} at DF and EDC averaged over 1000 years. See Methods for DF chronology and flux calculations. The EDC fluxes are plotted on the AICC12 timescale^{53,54} using previously published ion data^{7–9,16} and accumulation rates^{53,54}

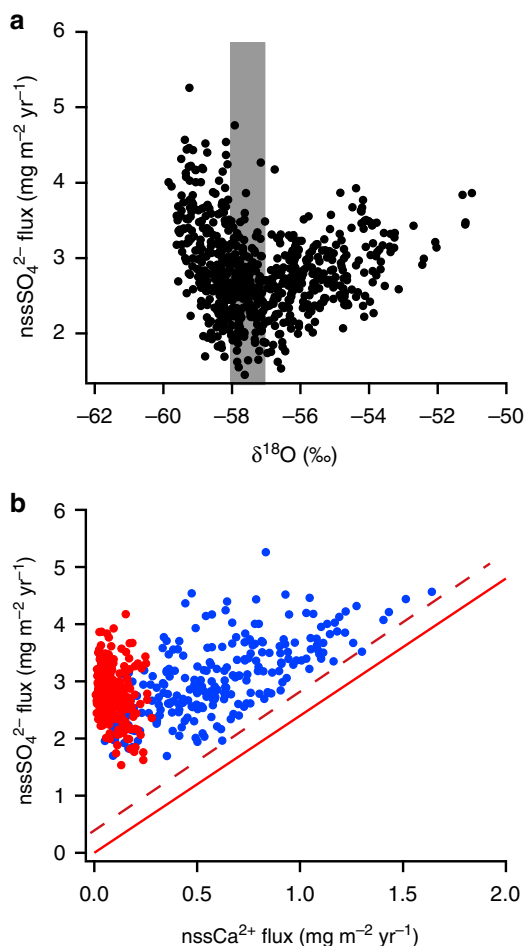


Fig. 2 Variability of nssSO_4^{2-} flux at Dome Fuji (DF). **a** DF nssSO_4^{2-} flux plotted against DF $\delta^{18}\text{O}$ ^{14,15}. Data points represent 1000-year averages. Before averaging, the $\delta^{18}\text{O}$ depths that differ from the ion data depths have been interpolated to match. Gray bar indicates the lower threshold of $\delta^{18}\text{O}$ (-58‰), below which the nssSO_4^{2-} flux decreases with $\delta^{18}\text{O}$, and the upper threshold (-57‰), above which the nssSO_4^{2-} flux increases with $\delta^{18}\text{O}$. **b** DF nssSO_4^{2-} flux plotted against DF nssCa^{2+} flux. Data points represent 1000-year averages. The slope of the solid red line ($m = 2.4$) represents the stoichiometric mass ratio of Ca/SO_4 as CaSO_4 . The dashed red line shows the lower bound of the nssSO_4^{2-} flux data with $m = 2.4$. Red and blue dots represent the data for warm and cold periods, respectively, corresponding to the $\delta^{18}\text{O}$ values above and below the thresholds

The dominant source of nssCa^{2+} is terrestrial dust^{7–9,16} and South America is a major source region for dust deposited in the Antarctic interior^{17–19}. Different nssCa^{2+} fluxes in three records can be explained by their different distances from the South American source region¹⁶. Contrary to previous studies on EDC and EDML cores, the nssSO_4^{2-} flux at DF is not constant (Figs. 1 and 2). The flux increases as $\delta^{18}\text{O}$ (a proxy for temperature at DF^{14,15}) decreases below approximately -58‰ , and increases when $\delta^{18}\text{O}$ is above approximately -57‰ .

Potential sources of nssSO_4^{2-} are marine biogenic DMS, volcanic sulphate, and terrestrial dust^{7,8}. With the exception of a few years following large volcanic eruptions, the volcanic input is estimated to be less than 10% of the present-day and Holocene sulphate budgets⁷. Oceanic DMS was previously regarded as the dominant nssSO_4^{2-} source over glacial/interglacial cycles, with only a small input from terrestrial sources^{7–9}. However, terrestrial sulphate can be a major source in glacials when the amount of dust increases. Fluxes of nssCa^{2+} and nssSO_4^{2-} at DF are

correlated during cold periods when $\delta^{18}\text{O}$ is below approximately -58‰ . The scatter plot of nssSO_4^{2-} against nssCa^{2+} (Fig. 2b) shows a lower bound whose slope is close to the stoichiometric ratio for CaSO_4 , indicating that a large proportion of nssSO_4^{2-} during cold periods exists as CaSO_4 . This same feature is reported for EDML and a similar but weaker correlation between nssCa^{2+} and nssSO_4^{2-} fluxes is reported for EDC²⁰. These observations suggest that a large proportion of nssSO_4^{2-} exists as CaSO_4 during cold periods at EDC and EDML²⁰, as well as DF. Micro-Raman spectroscopic analysis of DF samples from the Last Glacial Maximum (LGM) suggests that a large proportion of Ca^{2+} exists as gypsum ($\text{CaSO}_4 \cdot 2\text{H}_2\text{O}$)²¹. Furthermore, analyses of DF samples from the LGM using scanning electron microscopy/energy-dispersive X-ray spectroscopy (SEM-EDS) show that the majority of Ca^{2+} originates from CaSO_4 ²². Although the SEM-EDS analyses indicate that a large fraction of the particles consists of silicate minerals containing Ca, they do not dissolve in water. The majority of Ca^{2+} measured in this study using ion chromatography (see Methods) should therefore originate from CaSO_4 .

CaSO_4 in DF core could originate from two potential sources. First is primary gypsum, i.e., terrestrial gypsum transported from arid source regions as dust^{8,9,20,23}. Second is secondary gypsum formed by the reaction of CaCO_3 , one of the major components of terrestrial dust, with marine biogenic H_2SO_4 or SO_2 ^{20,24,25} during dust transport. If primary gypsum is dominant, the major source of nssSO_4^{2-} during cold periods should be dust, not marine biogenic sulphate. But if secondary gypsum is dominant, the major source of nssSO_4^{2-} should be marine biogenic sulphate. So far, secondary gypsum has been considered dominant, assuming limited fractions of terrestrial sulphate^{7,9,11}. A mean sediment $\text{SO}_4^{2-}/\text{Ca}^{2+}$ ratio of 0.1⁹ or 0.18 observed for soils^{10,12} is often referred to as a basis of a small terrestrial contribution. To define an uppermost limit,⁹ uses a ratio of 0.5 observed in Sharan dust plumes and suggests a maximum terrestrial contribution of only 16%. However, ratios are highly variable and source-dependent⁸.

Although the compositions of South American minerals are poorly documented, there is some evidence supporting the hypothesis that $\text{SO}_4^{2-}/\text{Ca}^{2+}$ ratios could be much higher than previously assumed. Soil samples from northeastern and central Patagonia, one of the potential source regions, show $\text{SO}_4^{2-}/\text{Ca}^{2+}$ ratios close to or larger than the stoichiometric ratio of CaSO_4 ^{26,27}. Because some of these soil samples have high $\text{Na}^+/\text{Ca}^{2+}$ and $\text{Mg}^{2+}/\text{Ca}^{2+}$ ratios (often much higher than 1), which is not the case for $\text{nssNa}^+/\text{nssCa}^{2+}$ and $\text{nssMg}^{2+}/\text{nssCa}^{2+}$ in the Antarctic ice samples (see [28] for $\text{nssNa}^+/\text{nssCa}^{2+}$ and Supplementary Discussion for $\text{nssMg}^{2+}/\text{nssCa}^{2+}$), such soils may not be the source for CaSO_4 in the Antarctic ice cores. However, high $\text{SO}_4^{2-}/\text{Ca}^{2+}$ ratios reported in Patagonia cast doubt on the assumption that the $\text{SO}_4^{2-}/\text{Ca}^{2+}$ ratio of 0.5 observed in Sharan dust plumes gives an uppermost limit⁹.

Gypsum is a major mineral in evaporites²⁹. A distribution of evaporites has been reported in wide regions of South America³⁰. Large areas of the Puna-Altiplano, one of the potential source regions of dust deposited in the Antarctic interior, are covered by salt-lake beds¹⁹, which could be sources of gypsum-rich evaporites, although the compositions of these lakes are poorly documented and could vary substantially²⁹. Giant evaporite belts dominated by halite and gypsum are also found in this region³¹. Puna evaporites are uniquely characterized by scarce carbonates, whereas sulphates and chlorides are abundant³¹. Furthermore, ion ratios $\text{nssCl}^-/\text{nssNa}^+$ and $\text{nssNa}^+/\text{nssCa}^{2+}$ estimated from EDC core suggest a significant contribution of halides mobilized from continental evaporite deposits²⁸. The reaction of CaCO_3 with H_2SO_4 and SO_2 is slow^{20,25,32,33}, and only a partial neutralization of clay or carbonate particles has been observed

even in areas where SO_2 and H_2SO_4 concentrations are greatly enhanced by volcanic contributions^{20,34}. If this can also be extended to the different conditions over the Southern Ocean, then terrestrial gypsum would be needed to explain the relationship between nssCa^{2+} and nssSO_4^{2-} in Antarctic ice cores and may be a major CaSO_4 source. To validate our idea, it will be important to establish what source areas could provide such a gypsum-rich source of dust.

Revised calculations of DMS-derived sulphate. To calculate the flux of DMS-derived nssSO_4^{2-} , the contribution of terrestrial sulphate should be removed. We first subtract the terrestrial nssSO_4^{2-} fraction as a case for a maximum contribution of terrestrial gypsum to nssSO_4^{2-} flux. Assuming that the majority of nssCa^{2+} originates from terrestrial sulphate and that nssCa^{2+} is a major terrestrial cation, we make a first-order estimate of the marine biogenic sulphate flux by subtracting the CaSO_4 contribution (nssCa^{2+} multiplied by 2.4, the stoichiometric mass ratio of SO_4/Ca for CaSO_4) from the total nssSO_4^{2-} flux. The residual nssSO_4^{2-} is thus dominated by sulphate in the form of H_2SO_4 and/or Na_2SO_4 . Both H_2SO_4 and Na_2SO_4 originate from DMS; the former is directly produced from DMS, whereas the latter is produced by the reaction between DMS-derived H_2SO_4 and NaCl ³⁵ (sea salt and/or terrestrial). The residual nssSO_4^{2-} flux, a revised marine biogenic sulphate flux, co-varies with the temperature proxy $\delta^{18}\text{O}$ at DF (Fig. 3) and displays high and low values during interglacials and cold periods in glacials, respectively. Similarly, residual nssSO_4^{2-} fluxes calculated for EDC and EDML show variability consistent with DF (Fig. 3). Opposite behaviors of marine biogenic and terrestrial sulphate would have led to small variability of the nssSO_4^{2-} flux over glacial/interglacial cycles. Larger dust input at DF and EDML owing to their proximity to the South American source regions relative to EDC (Fig. 1b, Supplementary Fig. 3a) would have resulted in greater variability in the nssSO_4^{2-} flux at DF and EDML compared with EDC (Fig. 1c, Supplementary Fig. 3b).

As stated above, we first subtract the terrestrial gypsum contribution to calculate the marine biogenic nssSO_4^{2-} flux. However, because nssSO_4^{2-} could have other sources, we perform a sensitivity test as follows. If a major fraction of nssSO_4^{2-} originates from evaporites, then other minerals commonly contained in evaporites could also contribute to the nssSO_4^{2-} flux. We take into account Mg^{2+} and K^+ , which could originate from evaporites and exist as sulphates²⁹, as well as the contribution of CaCO_3 , a major mineral in many of the dust source regions^{26,27} that likely reacts with HNO_3 or NO_x instead of H_2SO_4 or SO_2 due to faster reactions^{20,25,32,33,36} (Supplementary Discussion and Supplementary Fig. 4). Our conclusion that the residual nssSO_4^{2-} flux decreases during cold periods does not change, although the correlation between residual sulphate and temperature proxy changes slightly (Fig. 4a, b, Supplementary Fig. 5). We also change the $\text{nssSO}_4^{2-}/\text{nssCa}^{2+}$ ratio (R_1) assuming that part of CaSO_4 originates from the reaction of CaCO_3 with marine biogenic sulphate. When we change R_1 values, we consider only CaSO_4 and ignore other minerals. The same conclusion remains if $R_1 > 1.2$, but fails if $R_1 < 1.2$. For EDC and EDML cores, we consider only the CaSO_4 contribution because neither Mg^{2+} nor K^+ data are available.

We calculate the marine biogenic/total nssSO_4^{2-} ratio (R_2) for different terrestrial gypsum contributions (Supplementary Discussion and Supplementary Fig. 6). If we assume that Ca^{2+} and Mg^{2+} are major evaporite-originated cations that form sulphate in DF core and that the carbonate hosts of these ions react with HNO_3 or NO_x rather than H_2SO_4 or SO_2 , R_2 for the LGM is 0.46. This value is consistent with that estimated from sulphur isotopes

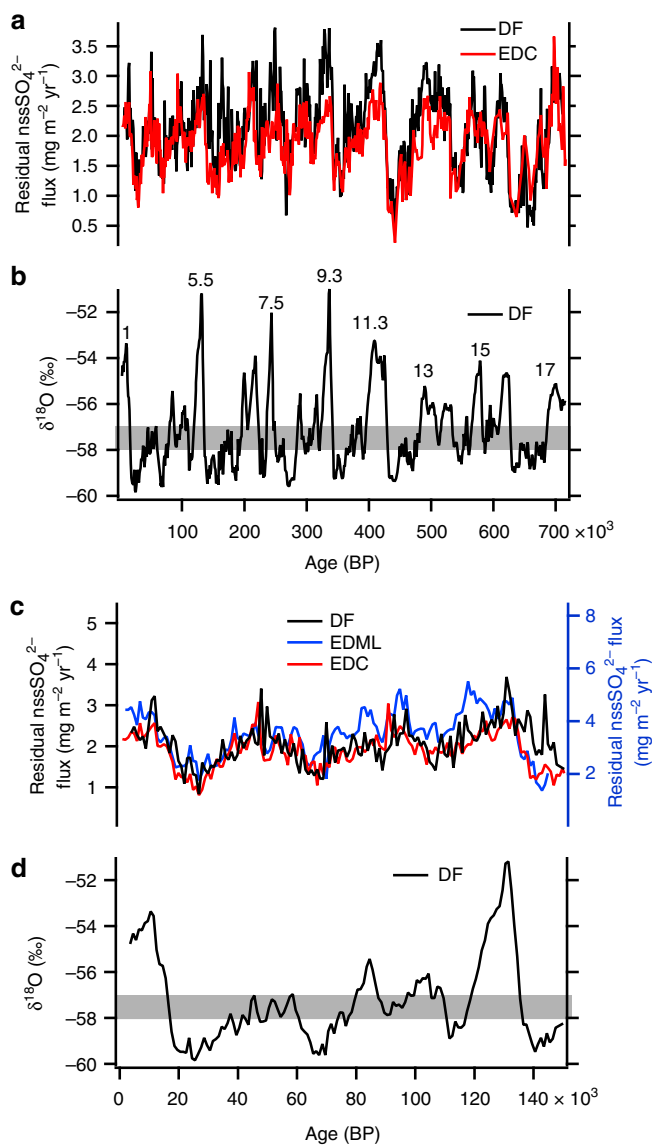


Fig. 3 Variability of residual nssSO_4^{2-} flux at Dome Fuji (DF), Dome C (EDC), and Dronning Maud Land (EDML). **a** Residual nssSO_4^{2-} flux at DF and EDC for the past 720,000 years, calculated by subtracting the terrestrial CaSO_4 contribution from the nssSO_4^{2-} flux. The EDC flux is plotted on the AICC12 timescale^{53,54} using previously published ion data^{7-9,16} and accumulation rates^{53,54}. **b** $\delta^{18}\text{O}$ at DF over the past 720,000 years^{14,15}. Gray bar indicates the thresholds (Fig. 2a). Marine isotope stage numbers for interglacials are also shown. **c** Residual nssSO_4^{2-} at DF, EDC, and EDML calculated by subtracting the terrestrial CaSO_4 contribution from the nssSO_4^{2-} flux. The EDC and EDML fluxes are plotted on the AICC12 timescale^{53,54} using previously published ion data^{7-9,16} and accumulation rates^{53,54}. **d** The $\delta^{18}\text{O}$ values at DF¹⁴ for the past 150,000 years. All ion and $\delta^{18}\text{O}$ values are averages over 1000 years

($R_2 \sim 0.5$) assuming no isotopic fractionation¹¹. However, R_2 values for interglacials exceed 1, which is implausible. This most likely suggests an overestimation of the NO_3^- derived from the reaction between carbonates and HNO_3 or NO_x , because NO_3^- can also exist as HNO_3 . If we consider only terrestrial gypsum as a major contributor to terrestrial nssSO_4^{2-} , $R_1 = 2.4, 1.5,$ and 1.3 yield $R_2 = 0.24, 0.52,$ and $0.59,$ respectively (Supplementary Fig. 6) for the LGM. The same R_1 values yield $R_2 = 0.36, 0.60,$ and $0.65,$ respectively, for EDC core, and $R_2 = 0.24, 0.56,$ and $0.60,$ respectively, for EDML core. Larger dust input at DF and

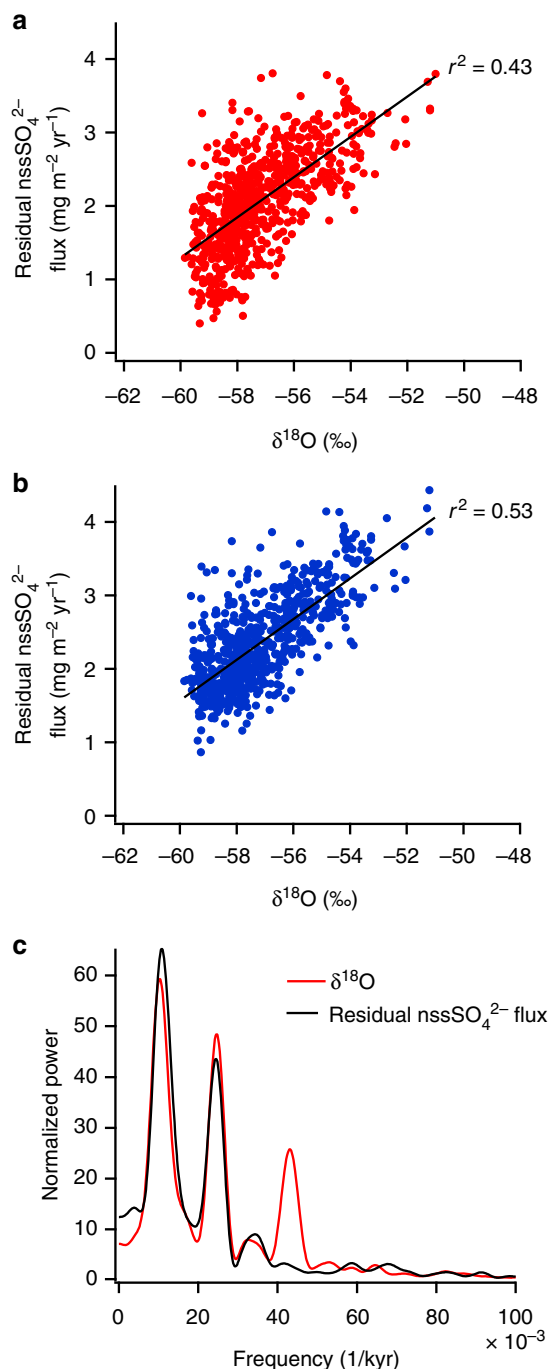


Fig. 4 Relationship between residual nssSO_4^{2-} flux and $\delta^{18}\text{O}$ at Dome Fuji (DF). **a** Residual nssSO_4^{2-} flux, considering only the terrestrial CaSO_4 contribution, plotted against $\delta^{18}\text{O}$ ^{14,15}. **b** Residual nssSO_4^{2-} flux considering the contributions of CaSO_4 , MgSO_4 , $\text{Ca}(\text{NO}_3)_2$, and $\text{Mg}(\text{NO}_3)_2$ plotted against $\delta^{18}\text{O}$ ^{14,15}. Residual nssSO_4^{2-} flux and $\delta^{18}\text{O}$ are averages over 1000 years. Before averaging, the $\delta^{18}\text{O}$ depths that differ from the ion data depths have been interpolated to match. Straight lines in **a** and **b** display results of linear regressions. Correlation coefficients (r) were calculated with sample size (n) = 681 and for significance level (α) = 0.05. **c** Normalized power spectra of residual nssSO_4^{2-} flux and $\delta^{18}\text{O}$ at DF. The residual nssSO_4^{2-} flux was calculated in the same manner as **b**. Power spectra were calculated with the Blackman-Tukey method (30% lag) using the AnalyseSeries software package⁵⁵ (see Methods). To use the software, the raw data were resampled to a 200-yr interval using linear interpolation

EDML likely yields smaller R_2 values compared with EDC. R_2 values for the LGM might be underestimated for large R_1 values (~2.4) owing to contribution of marine biogenic sulphate. In any case, a contribution of terrestrial sulphate during glacials is likely much larger than previously assumed, consistent with that estimated from sulphur isotope mass balance¹¹. This leads to a conclusion that DMS-derived sulphate decreases in glacials, although the degree of decrease remains uncertain depending on glacial/interglacial changes in R_2 values.

Reduced DMS emissions in the AZ of the SO during glacials.

Sulphate aerosol observations at EDC and coastal Antarctic sites display a clear seasonal pattern with a maximum in austral summer³⁷. High surface DMS concentrations and emission fluxes over the modern SO in austral summer have also been reported^{38,39}. The dominant source of biogenic sulphate in the Antarctic interior is thus most likely DMS emitted from the SO. The flux of marine biogenic sulphate deposited in the Antarctic interior would then be controlled by DMS emissions in the source regions, the location of these source regions (i.e., distance to Antarctic interior sites), DMS oxidation chemistry, and depositional processes. As glacial/interglacial changes in oxidation chemistry and deposition are likely to be small, the decreased biogenic sulphate flux during glacials would be caused by reduced DMS emissions and/or longer transport distances⁴⁰ (Supplementary Discussion). Transport distances depend strongly on the summer sea ice extent around Antarctica⁴⁰ (Supplementary Discussion), but only limited information is available for glacials. In the Indian Ocean sector, the summer sea ice extent at the LGM was only slightly greater than the present day⁴¹, whereas in the Atlantic Ocean sector, the sporadic occurrence of summer sea ice considerably farther north is indicated⁴¹ (Supplementary Discussion). Although data from other oceanic sectors are very sparse, Gersonde et al.⁴¹ speculate that the summer sea ice field around Antarctica changed from $4 \times 10^6 \text{ km}^2$ (present day) to $5\text{--}6 \times 10^6 \text{ km}^2$ (LGM).

DF and EDC display similar residual nssSO_4^{2-} fluxes with glacial/interglacial ratios of 1/3 to 1/4 (Fig. 3). The LGM/Holocene ratios (~1/3) at DF, EDC, and EDML are consistent with the MSA flux at Siple Dome (West Antarctica, Supplementary Fig. 1) where MSA can be used as a proxy for marine biogenic sulphur deposition because its post-depositional loss is minimal⁴². In other words, the four sites facing different sectors of the SO, which includes the Indian sector where summer sea ice extent increased only slightly at the LGM, display similar glacial/interglacial ratios of biogenic sulphur species. The similar ratios would be mainly associated with glacial-interglacial changes in DMS emissions in the SO, and specifically the AZ because it is a major DMS source region for biogenic sulphate in the present-day Antarctic interior^{38,43} (Supplementary Discussion). The reduced biogenic sulphate fluxes at the LGM could be partly due to the increased transport distances. However, the LGM increase in the summer sea ice extent around Antarctica by 1.25 to 1.50 times⁴¹ would only slightly increase the transport distances to the Antarctic interior sites, which are affected by a mixture of air masses from different oceanic sectors^{44,45} (Supplementary Discussion and Supplementary Fig. 7). Thus, lower biogenic nssSO_4^{2-} fluxes during glacials indicate reduced DMS emissions in the AZ, suggesting that primary production, as well as export production, decreases during glacials, which is consistent with marine sediment records⁴.

Discussion

Sea surface temperature (SST), solar radiation, sea ice extent, and nutrient and iron supply can affect DMS emissions^{1,43,46,47} in the

AZ. Power spectra of residual nssSO_4^{2-} show strong powers in the 41-kyr and 93-kyr bands (Fig. 4c). Powers in similar bands (41-kyr and 98-kyr) are also observed in the $\delta^{18}\text{O}$ record, which is closely linked to SST and sea ice extent in the AZ. To our knowledge, the relationship between DMS emissions and SST has not been directly investigated. The growth rate of phytoplankton (unicellular algae), however, shows little dependence on SST near the melting point of sea ice⁴⁸, which is the major source of DMS^{46,49}. Hence, covariance of the residual nssSO_4^{2-} flux and $\delta^{18}\text{O}$ record at DF (Figs. 3, 4, Supplementary Fig. 5) does not imply that decreased summer SST is a major cause of reduced DMS emissions. Although the integrated summer insolation at 55°S, the latitude of a major source region of DMS, shows strong spectral power in the 41-kyr band, variability in solar radiation could not be a major cause of the reduced DMS emissions during glacials because it is less than 3% (Supplementary Discussion). The large seasonal difference in sea ice extent during glacials implies large areas of melting sea ice in summer, which would lead to enhanced DMS emissions because melting sea ice is an important DMS source^{46,49}. However, this is not the case because DMS-derived sulphate decreases in glacials (Figs. 3, 4, Supplementary Fig. 5). Thus, the change in winter sea ice extent does not directly affect overall DMS emissions in the AZ on orbital timescales.

Vertical mixing and upwelling appear to dominate the nutrient and iron supply in Antarctic surface waters⁴. Expanded winter sea ice during glacials would enhance AZ stratification, weaken mixing and upwelling, and decrease the supply of nutrients and iron in winter⁴. This would decrease the nutrient/iron abundance and thus DMS emissions in summer. Reduced vertical mixing and upwelling during glacials should also reduce the CO_2 exchange between the ocean interior and atmosphere, thereby sequestering CO_2 into the ocean and leading to decreased atmospheric CO_2 concentrations, as is proposed by⁴. This study also implies that reduced DMS emissions during glacials may reduce cloud albedo, resulting in a negative feedback by biogenic sulphate aerosol-cloud interaction^{1,2}. Although an improved understanding of the precise mechanisms controlling nssSO_4^{2-} flux variations and their links to climate change is needed, the data provided here can be used to constrain the sulphur cycle and climate models. Ongoing analyses of sulphur isotopes of SO_4^{2-} ($\delta^{34}\text{S}$) in DF core will reduce the estimation uncertainty of DMS-derived sulphate, and enable more quantitative discussion on the interaction between DMS-derived sulphate and climate.

Methods

Ion data. We use ion data from DF1 and DF2 cores after and before 300,000 BP, respectively¹⁴. Na^+ , Ca^{2+} , Mg^{2+} , NO_3^- , and SO_4^{2-} were measured from both cores using ion chromatography. In addition, K^+ was measured from DF2 core. For DF1 core, we use previously published data⁵⁰ after re-examination and removal of some data points because of large measurement errors. Fifty-nine samples were newly cut from DF1 core, re-measured, and the new data were added to the earlier dataset. Measurement errors were generally less than 10% but may be higher for low concentrations. For DF2 core, 10-cm-long samples were cut every 0.5 m and measured on two Dionex DX-500 ion chromatographs: one for anions and the other for cations. Measurement errors were estimated to be less than 3%. Sea salt (ss) Na^+ and non-sea-salt (nss) Ca^{2+} concentrations were calculated from Na^+ and Ca^{2+} concentration data using the weight ratios of $\text{Ca}^{2+}/\text{Na}^+$ for seawater (0.038) and average crust (1.78), as described in previous studies^{7–9,16,51}. The nssSO_4^{2-} concentrations were calculated assuming a sea ice source^{7,8} of ss Na^+ . Similar values are obtained if we assume an open ocean source^{7,8} of ss Na^+ . Fluxes of nss Ca^{2+} and nssSO_4^{2-} were calculated by multiplying concentrations by estimated accumulation rates¹⁴.

Chronology and accumulation rate estimation. We use the DFO-2006⁵² timescale for the past ~342,000 years and the AICC2012⁵³ timescale for the period older than ~344,000 years¹⁴. The AICC2012^{53,54} chronology is used for EDC and EDML. The accumulation rates at DF were deduced from the $\delta^{18}\text{O}$ record by Dome Fuji Community members¹⁴, and those at EDC and EDML were taken from [53,54].

Spectral analysis. Spectral analyses were carried out with the AnalyseSeries software package⁵⁵ (Fig. 4c). Blackman-Tukey spectra (30% lag) using a Bartlett window with a bandwidth of 0.00702905 are shown in Fig. 4c. The amplitudes of the spectra were normalized. The $\delta^{18}\text{O}$ and residual nssSO_4^{2-} data used for the spectral analysis were resampled at a 200-yr interval using linear interpolation. For resampling, $\delta^{18}\text{O}$ data from¹⁴ and residual nssSO_4^{2-} data provided in the Source Data file were used.

Data availability

The source data underlying Figs. 1–4 and Supplementary Figs. 2–7 are provided as a Source Data file. The data are also available in the Arctic and Antarctic Data Archive System at the National Institute of Polar Research [<https://ads.nipr.ac.jp/dataset/A20190607-001>].

Received: 10 June 2018 Accepted: 24 June 2019

Published online: 19 July 2019

References

1. Charlson, R. J., Lovelock, J. E., Andreae, M. O. & Warren, S. G. Oceanic phytoplankton, atmospheric sulphur, cloud albedo and climate. *Nature* **326**, 655–661 (1987).
2. Carslaw, K. S. et al. Large contribution of natural aerosols to uncertainty in indirect forcing. *Nature* **503**, 67–71 (2013).
3. IPCC, 2013: Climate Change 2013: The Physical Science Basis. In *Contribution of Working Group I to the Fifth Assessment Report of the Intergovernmental Panel on Climate Change* (eds Stocker, T. F. et al.). (Cambridge University Press, Cambridge, UK, 2013).
4. Jaccard, S. L. et al. Two modes of change in Southern Ocean productivity over the past million years. *Science* **339**, 1419–1423 (2013).
5. Legrand, M. R., Delmas, R. K. & Charlson, R. J. Climate forcing implications from Vostok ice-core sulphate data. *Nature* **335**, 418–420 (1988).
6. Legrand, M. et al. Ice-core record of oceanic emissions of dimethylsulphide during the last climate cycle. *Nature* **350**, 144–146 (1991).
7. Wolff, E. W. et al. Southern Ocean sea-ice extent, productivity and iron flux over the past eight glacial cycles. *Nature* **440**, 491–496 (2006).
8. Wolff, E. W. et al. Changes in environment over the last 800,000 years from chemical analysis of the EPICA Dome C ice core. *Quat. Sci. Rev.* **29**, 285–295 (2010).
9. Kaufmann, P. et al. Ammonium and non-sea salt sulfate in the EPICA ice cores as indicators of biological activity in the Southern Ocean. *Quat. Sci. Rev.* **29**, 313–323 (2010).
10. Patris, N. et al. First sulfur isotope measurements in central Greenland ice cores along the preindustrial and industrial periods. *J. Geophys. Res. Atmos.* **107**, ACH 6-1–ACH 6-11 (2002).
11. Alexander, B. et al. East Antarctic ice core sulfur isotope measurements over a complete glacial-interglacial cycle. *J. Geophys. Res. Atmos.* **108**, <https://doi.org/10.1029/2003JD003513> (2003).
12. Kunasek, S. A. et al. Sulfate sources and oxidation chemistry over the past 230 years from sulfur and oxygen isotopes of sulfate in a West Antarctic ice core. *J. Geophys. Res. Atmos.* **115**, <https://doi.org/10.1029/2010JD013846> (2010).
13. Uemura, R. et al. Sulfur isotopic composition of surface snow along a latitudinal transect in East Antarctica. *Geophys. Res. Lett.* **43**, 5878–5885 (2016).
14. Dome Fuji Ice Core Project members. State dependence of climatic instability over the past 720,000 years from Antarctic ice cores and climate modeling. *Sci. Advances* **3**, <https://doi.org/10.1126/sciadv.1600446> (2017).
15. Uemura, R. et al. Asynchrony between Antarctic temperature and CO_2 associated with obliquity over the past 720,000 years. *Nature Comm.* **9**, <https://doi.org/10.1038/s41467-018-03328-3> (2018).
16. Fischer, H. et al. Reconstruction of millennial changes in dust emission, transport and regional sea ice coverage using the deep EPICA ice cores from the Atlantic and Indian Ocean sector of Antarctica. *Earth Planet. Sci. Lett.* **260**, 340–354 (2007).
17. Delmonte, B. et al. Comparing the Epica and Vostok dust records during the last 220,000 years: stratigraphical correlation and provenance in glacial periods. *Earth-Sci. Rev.* **66**, 63–87 (2004).
18. Gaiero, D. M. Dust provenance in Antarctic ice during glacial periods: from where in southern South America? *Geophys. Res. Lett.* **34**, L17707 (2007).
19. Gili, S. et al. Glacial/interglacial changes of Southern Hemisphere wind circulation from the geochemistry of South American dust. *Earth. Planet. Sci. Lett.* **469**, 98–109 (2017).
20. De Angelis, M., Traversi, R. & Udisti, R. Long-term trends of mono-carboxylic acids in Antarctica: comparison of changes in sources and transport processes at the two EPICA deep drilling sites. *Tellus B Chem. Phys. Meteorol.* **64**, 1–21 (2012).

21. Sakurai, T. et al. The chemical forms of water-soluble microparticles preserved in the Antarctic ice sheet during Termination I. *J. Glaciol.* **57**, 1027–1032 (2011).
22. Iizuka, Y. et al. Constituent elements of insoluble and non-volatile particles during the Last Glacial Maximum exhibited in the Dome Fuji (Antarctica) ice core. *J. Glaciol.* **55**, 552–562 (2009).
23. Rojas, C. M. et al. The elemental composition of airborne particulate matter in the Atacama desert, Chile. *Sci. Total Environ.* **91**, 251–267 (1990).
24. Legrand, M. R., Lorius, C., Barkov, N. I. & Petrov, V. N. Vostok (Antarctica) ice core: Atmospheric chemistry changes over the last climatic cycle (160,000 years). *Atmos. Environ.* **22**, 317–331 (1988).
25. Usher, C. R., Michel, A. E. & Grassian, V. H. Reactions on mineral dust. *Chem. Rev.* **103**, 4883–4940 (2003).
26. Bouza, P. J., Simón, M., Aguilar, J., del Valle, H. & Rostagno, M. Fibrous-clay mineral formation and soil evolution in Aridisols of northeastern Patagonia, Argentina. *Geoderma* **139**, 38–50 (2007).
27. Bouza, P., Valle, H. F. & Del Imbellone, P. A. Micromorphological, physical, and chemical characteristics of soil crust types of the central Patagonia region, Argentina. *Arid Soil Res. Rehab.* **7**, 335–368 (1993).
28. Bigler, M., Röthlisberger, R., Lambert, F., Stocker, T. F. & Wagenbach, D. Aerosol deposited in East Antarctica over the last glacial cycle: Detailed apportionment of continental and sea-salt contributions. *J. Geophys. Res.* **111**, <https://doi.org/10.1029/2005jd006469> (2006).
29. Babel, M. & Schreiber, B. C. Geochemistry of evaporites and evolution of seawater. In *Treatise on Geochemistry*, 2nd Edition (eds Holland, H. D. & Turekian, K. K.) 483–560 (Elsevier, Amsterdam, 2014).
30. Drewry, G. E., Ramsay, A. T. S. & Smith, A. G. Climatically controlled sediments, geomagnetic-field, and trade wind belts in Phanerozoic time. *J. Geol.* **82**, 531–553 (1974).
31. Alonso, R. N., Jordan, T. E., Tabbutt, K. T. & Vandervoort, D. S. Giant evaporite belts of the Neogene central Andes. *Geology* **19**, 401–404 (1991).
32. Ooki, A. & Uematsu, M. Chemical interactions between mineral dust particles and acid gases during Asian dust events. *J. Geophys. Res. Atmos.* **10**, <https://doi.org/10.1029/2004JD004737> (2005).
33. Sullivan, R. C., Guazzotti, S., Sodeman, D. A. & Prather, K. A. Direct observations of the atmospheric processing of Asian mineral dust. *Atmos. Chem. Phys.* **7**, 1213–1236 (2007).
34. Carrico, C. M., Kus, P., Rood, M. J., Quinn, P. K. & Bates, T. S. Mixtures of pollution, dust, sea salt, and volcanic aerosol during ACE-Asia: Radiative properties as a function of relative humidity. *J. Geophys. Res. Atmos.* **108**, <https://doi.org/10.1029/2003JD003405> (2003).
35. Legrand, M. R. & Delmas, R. J. Formation of HCl in the Antarctic atmosphere. *J. Geophys. Res. Atmos.* **93**, 7153–7168 (1988).
36. Pan, X. et al. Real-time observational evidence of changing Asian dust morphology with the mixing of heavy anthropogenic pollution. *Sci. Rep.* **7**, 335 (2017).
37. Preunkert, S. et al. Seasonality of sulfur species (dimethyl sulfide, sulfate, and methanesulfonate) in Antarctica: inland versus coastal regions. *J. Geophys. Res.* **113**, D15302, <https://doi.org/10.1029/2008JD009937> (2008).
38. Kettle, A. J. et al. A global database of sea surface dimethylsulfide (DMS) measurements and a procedure to predict sea surface DMS as a function of latitude, longitude, and month. *Glob. Biogeochem. Cycles* **13**, 399–444 (1999).
39. Lana, A. et al. An updated climatology of surface dimethylsulfide concentrations and emission fluxes in the global ocean. *Glob. Biogeochem. Cycles* **25**, GB1004 (2011).
40. Castebrunet, H., Genthon, C. & Martinerie, P. Sulfur cycle at Last Glacial Maximum: model results versus Antarctic ice core data. *Geophys. Res. Lett.* **33**, L22711 (2006).
41. Gersonde, R., Crosta, X., Abelmann, A. & Armand, L. Sea-surface temperature and sea ice distribution of the Southern Ocean at the EPILOG Last Glacial Maximum—a circum-Antarctic view based on siliceous microfossil records. *Quat. Sci. Rev.* **24**, 869–896 (2005).
42. Saltzman, E. S., Dioumaeva, I. & Finley, B. D. Glacial/interglacial variations in methanesulfonate (MSA) in the Siple Dome ice core, West Antarctica. *Geophys. Res. Lett.* **33**, L11811 (2006).
43. Jarnikova, T. & Tortell, P. D. Towards a revised climatology of summertime dimethylsulfide concentrations and sea-air fluxes in the Southern Ocean. *Environ. Chem.* **13**, 364–378 (2016).
44. Suzuki, K., Yamanouchi, T. & Motoyama, H. Moisture transport to Syowa and Dome Fuji stations in Antarctica. *J. Geophys. Res.* **113**, D24114 (2008).
45. Suzuki, K., Yamanouchi, T., Kawamura, K. & Motoyama, H. The spatial and seasonal distributions of air-transport origins to the Antarctic based on 5-day backward trajectory analysis. *Polar Sci.* **7**, 205–213 (2013).
46. Abram, N. J., Wolff, E. W. & Curran, M. A. J. A review of sea ice proxy information from polar ice cores. *Quat. Sci. Rev.* **79**, 168–183 (2013).
47. Gabric, A. J., Cropp, R., Hirst, T. & Marchant, H. The sensitivity of dimethyl sulfide production to simulated climate change in the eastern Antarctic Southern Ocean. *Tellus B Chem. Phys. Meteorol.* **55**, 966–981 (2003).
48. Eppley, R. W. Temperature and phytoplankton growth in the sea. *Fish. Bull.* **70**, 1068–1085 (1972).
49. Nomura, D., Kasamatsu, N., Tateyama, K., Kudoh, S. & Fukuchi, M. DMSP and DMS in coastal fast ice and under-ice water of Lutzow-Holm Bay, eastern Antarctica. *Cont. Shel. Res.* **31**, 1377–1383 (2011).
50. Watanabe, O. et al. General trends of stable isotopes and major chemical constituents of the Dome Fuji deep ice core. *Mem. Natl. Inst. Polar Res. Spec. Issue No 57*, 1–24 (2003).
51. Röthlisberger, R. et al. Dust and sea salt variability in central East Antarctica (Dome C) over the last 45 kyrs and its implications for southern high-latitude climate. *Geophys. Res. Lett.* **29**, 1963 (2002).
52. Kawamura, K. et al. Northern Hemisphere forcing of climatic cycles in Antarctica over the past 360,000 years. *Nature* **448**, 912–916 (2007).
53. Bazin, L. et al. An optimized multi-proxy, multi-site Antarctic ice and gas orbital chronology (AICC2012): 120–800 ka. *Clim. Past* **9**, 1715–1731 (2013).
54. Veres, D. et al. The Antarctic ice core chronology (AICC2012): an optimized multi-parameter and multi-site dating approach for the last 120 thousand years. *Clim. Past* **9**, 1733–1748 (2013).
55. Paillard, D., Labeyrie, L. & Yiou, P. Macintosh program performs time-series analysis. *Eos Trans. Am. Geophys. Union* **77**, 379 (1996).

Acknowledgements

We thank the Dome Fuji Deep Ice Core Project members who contributed to the ice coring and ice core processing. The Japanese Antarctic Research Expedition (JARE), managed by the Ministry of Education, Culture, Sports, Science and Technology (MEXT), provided primary logistical support for the Dome Fuji Deep Ice Core Project. We thank Eric Wolff and Hubertus Fischer who provided the EDC and EDML ion data and valuable comments on the manuscript. We thank Yutaka Tobo for discussions regarding the chemical reactions of mineral aerosols, and two reviewers for their constructive comments. We also thank Yoshimi Ogawa-Tsukagawa for her help in drawing diagrams. This study was supported in part by MEXT (Grant-in-Aid for Scientific Research 15101001, 21221002, 15H01731, and 17H06316) and National Institute of Polar Research (Project Research KP305).

Author contributions

H.M. and Y.F. recovered the Dome Fuji cores. K.G.-A., M.H., T.M., T.K., R.U., K.S., Y.I., T. Suzuki, S. Horikawa, and K.F. processed the cores. M.H. and M.I. performed ion analyses. R.U. and H.M. obtained stable isotope data. T.K., M.H., and K.G.-A. were responsible for quality control of the ion data. K.G.-A. led the manuscript preparation. R.U., T. Suzuki, T. Sakurai, and K.F. contributed to the discussion on the ice core data. Y.K. contributed to the discussion on DMS and overall manuscript preparation. S. Hattori contributed to the discussion on sulphur isotopes.

Additional information

Supplementary Information accompanies this paper at <https://doi.org/10.1038/s41467-019-11128-6>.

Competing interests: The authors declare no competing interests.

Reprints and permission information is available online at <http://npg.nature.com/reprintsandpermissions/>

Peer review information: *Nature Communications* thanks Eric Wolff and other anonymous reviewer(s) for their contribution to the peer review of this work. Peer reviewer reports are available.

Publisher's note: Springer Nature remains neutral with regard to jurisdictional claims in published maps and institutional affiliations.



Open Access This article is licensed under a Creative Commons Attribution 4.0 International License, which permits use, sharing, adaptation, distribution and reproduction in any medium or format, as long as you give appropriate credit to the original author(s) and the source, provide a link to the Creative Commons license, and indicate if changes were made. The images or other third party material in this article are included in the article's Creative Commons license, unless indicated otherwise in a credit line to the material. If material is not included in the article's Creative Commons license and your intended use is not permitted by statutory regulation or exceeds the permitted use, you will need to obtain permission directly from the copyright holder. To view a copy of this license, visit <http://creativecommons.org/licenses/by/4.0/>.

© The Author(s) 2019